Histone H4 limits transcription of the histone locus in Drosophila

Kami Ahmad[1]*, Matt Wooten[1], Brittany N Takushi[1], Velinda Vidaurre[2], Xin Chen[2,3] & Steven Henikoff[1,3]*

[1]Basic Science Division, Fred Hutchinson Cancer Center, Seattle, WA, USA
[2]Department of Biology, The Johns Hopkins University, Baltimore, Baltimore, MD, USA
[3]Howard Hughes Medical Institute, Chevy Chase, MD, USA

*Corresponding authors: kahmad@fredhutch.org, steveh@fredhutch.org

Abstract

The expression of core histone genes is coupled to DNA replication of the genome to support chromatin packaging. In Drosophila, core histone genes are repeated in one locus as a 100-copy array and forms the Histone Locus Body; these multiple copies support varying rates of cell proliferation in different developmental stages and various tissues of the animal. We show here that the Drosophila Histone Locus Body contains a mix of active and silenced units. In the male germline reporter histone repeat units are strongly silenced, and we used this setting to test the dependence of expression on chromatin factors and histones. We find that silenced histone genes are induced in response to demand for histones, and from a selected survey we identify that only the H4 histone is required for reporter silencing. Further, histone H4 protein localizes to the Histone Locus Body and is most enriched immediately after S phase of the cell cycle. This argues for a role of histone H4 in coupling the demand for histones for chromatin packaging to histone gene expression. Binding patterns of the NPAT regulatory factor and RNA Polymerase II in K562 cells suggests that this regulatory principle also operates in human cells.

Author Summary

Cell proliferation in eukaryotes requires the coordination of DNA replication to duplicate the genome and synthesis of new histones to package that DNA. *Drosophila melanogaster* has a single array of histone genes, where some are actively transcribed and others are silenced. Here, we present evidence that the number of activated genes responds to the demand for histones during DNA replication. We identify one histone protein as a factor that localizes to the histone gene array, and that reduced levels of this histone induce the expression of otherwise silenced histone genes. In human cells, the gene encoding this same histone is the predominant target for activating transcription proteins, and is expressed more highly than other histones. The amount of this one histone may serve to sense the demand for histones during DNA replication, so that increased levels of this histone when DNA replication is complete represses histone gene expression.

Introduction

The genome of eukaryotic cells is packaged into nucleosomes, where DNA is wrapped around histone octamers. In animal cells, the genes encoding histone proteins are distinctive; most histone is produced from a set of repeated genes that are strongly induced during S phase of the cell cycle, and produce transcripts that lack introns and 3' poly-adenylation [Duronio & Marzluff 2017]. These genes nucleate a distinctive nuclear body within the nucleus termed the Histone Locus Body (HLB), where specific transcription factors and RNA processing proteins localize. In Drosophila, the single histone locus on Chromosome 2 contains ~100 copies of a histone repeat unit with a gene for histone H4, histone H3, histone H2A, histone H2B, and histone H1, and the two histone loci in diploid cells associate in one HLB [Liu et al 2006]. It has been unclear how many of these 200 genes are transcribed, because repetitive sequences in Drosophila are usually subject to heterochromatic silencing [Elgin 1996]. Further, the demand for histone gene expression varies between rapidly and slowly proliferating cell types, and genetic experiments have shown that flies are viable and fertile with an array of as few as 8 or 12 histone repeat units [Günesdogan et al 2010; MacKay et al 2015]. This suggests that many of the histone genes in wildtype flies are silenced, and only a few in the locus are expressed.

To address this, we profiled RNA Polymerase II (RNAPII) binding and histone modifications at histone gene in wildtype flies and flies with only 12 histone repeat units, where all units must be active. From these results, we infer that silenced histone genes are marked with histone H3 lysine-9 mono- and di-methylation (H3K9me1 and H3K9me2). Using marked reporter histone repeat units, we show that extra histone genes are silenced in wildtype animals, but are induced in genotypes with reduced histone gene numbers. Silencing of histone genes is most extreme in the male germline, and we used this setting to explore the genetic dependencies of histone gene silencing. Surprisingly, we find that histone gene silencing is modulated by the levels of one and only one histone: histone H4. This implies a direct mechanism whereby available histone H4 in cells buffers histone gene transcription to coordinate chromatin

packaging with DNA replication.

Results

Chromatin features at active and silenced histone genes in Drosophila

As the histone genes in the histone locus body (HLB) are repetitive, and normal cells contain both active and silenced histone genes, mapping of chromatin features to a genome assembly cannot distinguish which features are associated with which expression state. To address this, we profiled chromatin features in two genotypes: wildtype, where some of the ~200 histone genes must be active while others are silenced, and the "12XWT" line, where the histone locus has been deleted and a construct carrying 12 copies of the histone repeat unit (HRU) rescues the flies [Crain et al 2024]. We expect all copies of the histone genes to be active in this second genotype. By comparing chromatin profiles between these two genotypes, we infer the chromatin features of active and of silenced histone genes.

We dissected wing imaginal discs from male larvae as a sample of proliferating cells, and subjected them to CUT&Tag profiling [Kaya-Okur et al 2019], generating >1 million reads mapped to the dm6 genome assembly for each sample (**Supplementary Table 1**). We first used antibodies to the HLB-specific transcription factor Mxc [White et al 2011] and the transcriptional cofactor Mute [Bulchand et al 2010]. As expected, these two factors are localized to only the histone locus in the genome (**Figure 1a**). Signal for both factors is broadly dispersed across the *His3-His4* and *His2A-His2B* gene pairs of the 5 kb HRU, with peaks at the divergent promoters of each pair, and no signal over the adjacent *His1* gene (**Figure 1b**). The divergent *His4-His3* promoter region nucleates HLB formation [Salzler et al 2013], and these binding profiles are consistent with the idea that Mxc binds at these sites in the histone locus and nucleates HLB formation.

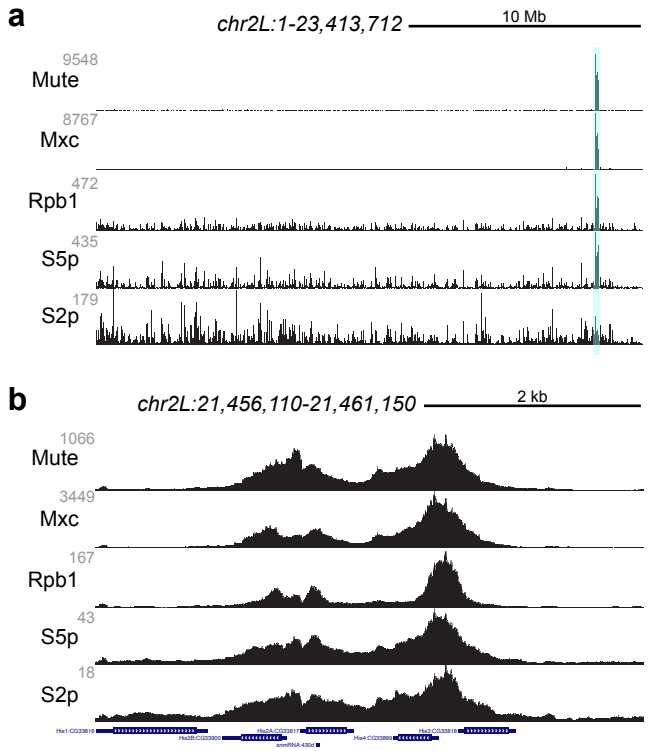

Figure 1. Chromatin factors and RNAPII at the histone locus in wing imaginal disc cells. (a) Browser tracks of chromatin factors and RNAPII isoforms across chromosome 2L of the dm6 assembly. Grey numbers indicate maximum normalized signal for each window. Blue shading marks the histone locus. **(b)** Browser tracks of chromatin factors and RNAPII isoforms across one instance of the 5 kb HRU.

To assess transcriptional activity of the histone genes, we profiled multiple components and isoforms of RNA polymerase II in larval wing disc samples. As expected, the RNAPII component unphosphorylated Rpb1, and phosphorylated initiating (RNAPII-S5p) and elongating (RNAPII-S2p) isoforms of Rpb1 mark the histone locus in wildtype cells (**Figure 1**). In fact, the histone locus is the major site of Rpb1 and RNAPII-S5p signal across the genome (**Figure 1a**), accounting for 1.8% and 2.5% of mapped reads, respectively, while only 0.2% of reads for RNAPII-S2p map to this locus. This is consistent with cytological description of enrichment for the unmodified and initiating forms of RNAPII at the HLB in other Drosophila cell types [Huang et al 2021, Lu et al 2024]. Note that the *His3-His4* and *His2A-His2B* have strong peaks of RNAPII-S5p and RNAPII-S2p at their promoters and across their gene bodies, indicating high transcription of these genes. In contrast, *His1* has only a low broad distribution of these polymerase isoforms across its length (**Figure 1b**), implying that it is expressed at lower levels.

We then compared signal counts for Mxc, Mute, and RNAPII between wing disc samples from wildtype and from *12XWT* flies. The sum counts of Mute and Mxc signal are higher in wildtype than in 12X flies, and proportional to the numbers of histone genes in these genotypes (**Table 1**). In contrast, signals for RNAPII-S5p are dramatically increased, and signal for RNAPII-S2p shows a slight gain. Adjusting for the number of histone genes in each genotype, each histone gene in the 12XWT line must carry more RNAPII than in wildtype. This is consistent with the idea that some histone genes are active and others silenced in wildtype, but all histone genes in the 12XWT strain must be active to support cell proliferation, and in fact appear to be more heavily transcribed.

Table 1. Enrichment of chromatin factors and histone modifications at replication-dependent histone genes in wild-type and 12XWT wing imaginal disc cells.

	Mxc	Mute	RNAPII-S5p	RNAPII-S2p	H3K9me1	H3K9me2	H3K9me3	H3K27me3	uH2A	H3K4me1	H3K4me2	H3K4me3	H3K27ac	H3K36me3
log2(CPM)	18.50	18.84	14.00	11.48	12.56	10.51	9.70	9.36	11.21	11.63	13.10	12.92	11.06	9.15
His1	1.31	1.78	4.12	2.17	-0.57	0.95	2.11	0.56	2.21	0.61	2.46	3.91	2.00	3.02
His2A	-0.05	0.73	3.47	1.59	-1.23	-1.23	1.44	0.39	1.05	-0.38	1.77	3.12	1.32	1.19
His2B	0.40	1.05	3.81	2.03	-0.73	-1.11	1.60	0.86	1.87	0.31	2.29	3.34	1.77	2.02
His3	0.06	0.87	3.95	1.93	-1.00	-0.94	-0.05	0.99	1.43	0.16	1.99	3.06	0.94	1.97
His4	0.33	0.95	4.21	2.40	-0.82	-2.48	1.70	1.34	1.61	0.16	1.81	3.07	1.52	2.09

Heterochromatic histone marks at silenced HLB genes

We first profiled histone modifications associated with active gene expression [Barth & Imhof 2010]. In most cases these reflect the expected activities of the histone genes in wildtype and 12XWT flies. There is little detectable trimethylation of the K36 residue of histone H3 (H3K36me3) in wildtype samples (**Figure 2**), consistent with the intronless structure of histone genes [Schwartz et al 2009], and this lack is unaffected in 12XWT samples (**Table 1**). In contrast, all three methylation states of the histone H3K4 residue (H3K4me1, H3K4me2, and H3K4me3) and acetylation at histone H3-K27 (H3K27ac) are enriched at the wildtype histone locus at levels comparable to surrounding active enhancers and genes (**Figure 2**). Accounting for copy number, there is a substantial gain only in H3K4me3 in the 12XWT line (**Table 1**), consistent with higher average transcription of each gene.

We then examined five histone modifications typically associated with silencing across histone genes between the two Drosophila lines. Three modifications are found at the histone genes in wildtype samples: mono- and di-methylation of histone H3 at lysine-9 (H3K9me1 and H3K9me2 [Ebert et al 2006]), and ubiquitinylation of histone H2A at lysine-118 (uH2A [Barbour et al 2020]) (**Figure 2a**). These first two marks imply that histone genes have a partially heterochromatic character, although this locus lacks the more silencing tri-methylation of histone H3 at lysine-9 (H3K9me3 [Ebert et al 2006]) (**Figure 2a**). The presence of uH2A at histone genes suggests that these are sites of PRC1 activity, although the canonical trimethylation mark of histone H3 at lysine-27 (H3K27me3 [Cao et al 2002]) mark of Polycomb-silenced domains is absent.

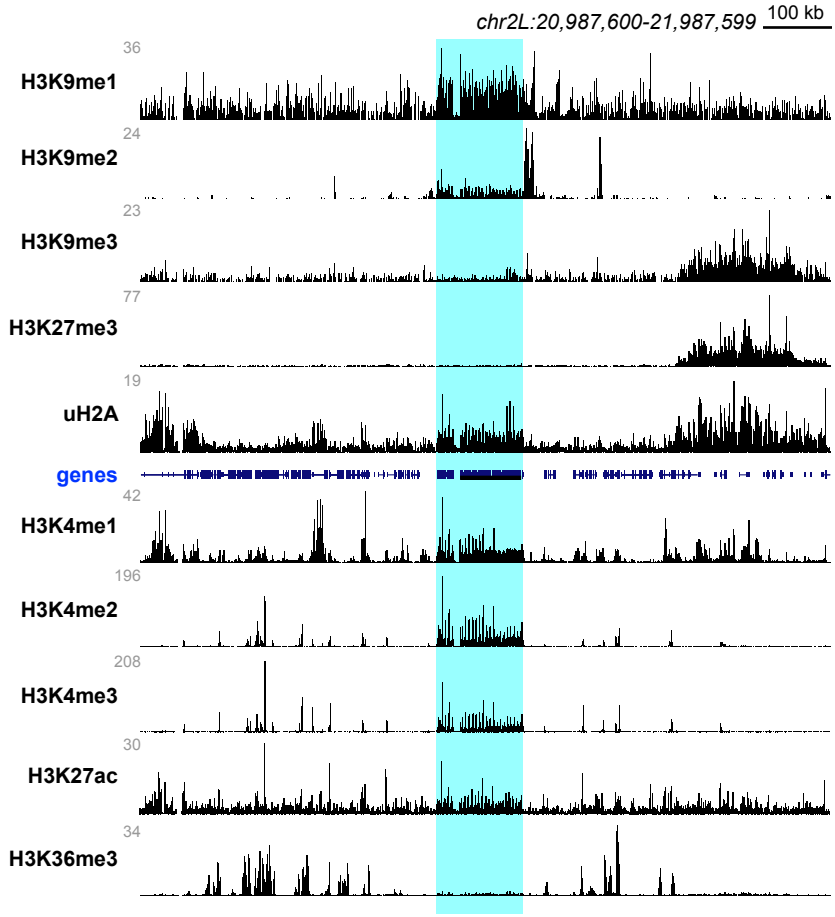

Figure 2. Histone modifications at the histone locus in wildtype. Browser tracks of histone modifications around the histone locus in the dm6 assembly. Blue shading marks the histone locus.

Any histone modifications associated with silencing should be present at histone genes in wildtype, but absent in the 12XWT line. Previous results have implicated H3K9 methylation in histone gene silencing [Ner et al 2002; Ito et al 2012]. Indeed, the densities of H3K9me1 and H3K9me2 drop in the 12XWT strain compared to wildtype, and these reductions are greater than expected from the difference in gene copy number (**Table 1**). In contrast, the change in uH2A density is similar to that expected from the copy number change. These results support the idea that inactive histone genes are marked for heterochromatic silencing at the H3K9 residue.

Extreme silencing of the HLB in Drosophila stem/progenitor cells

To visualize histone gene expression in living animals, we used HRU reporter constructs where either the *His3* or the *His2A*

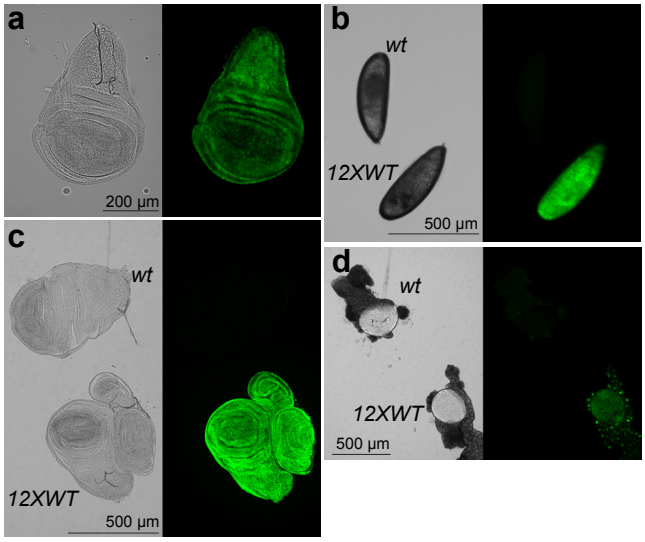

Figure 3. Expression of a *His2ADendra2* reporter HRU in wildtype and 12XWT HRU strains. (a) Fluorescence of the *His2ADendra2* reporter in a wildtype larval wing disc. **(b)** Fluorescence of *His2ADendra2* in larval wing imaginal discs from wildtype (wt) and from 12XWT larvae. **(c)** Fluorescence of *His2ADendra2* in embryos from wildtype (wt) and from 12XWT lines. **(d)** Fluorescence of *His2ADendra2* in testes and associated fat body from wildtype (wt) and from 12XWT larvae.

gene is fused to the octocoral *Dendra2* fluorescent protein coding sequence [Shindo & Amodeo 2019; **Methods**]. These constructs express fluorescently tagged histones in eggs and developing embryos [Shindo & Amodeo 2019], and at low levels in proliferating cells of later stages such as in larval imaginal wing discs (**Figure 3a**). We reasoned that if histone genes are derepressed when their copy number is reduced, a marked ectopic HRU would express more tagged protein in the 12XWT background. Indeed, the expression of a tagged HRU is dramatically increased by ~200-fold in developing embryos (**Figure 3b**), and in larval tissues (**Figure 3c,d**). This implies that cells with this reduced histone gene background sense a dearth of histones, and hypertranscribe all remaining histone genes to provide for chromatin duplication.

The amount of Dendra2-tagged histone varies between tissues, and is noticeably low in the testes of male larvae (**Figure 3d**). We used this setting to examine HRU reporter expression in more detail. The adult testis is a curled tube structure where germline stem cells located at the apical tip of the testis undergo four rounds of mitotic division producing spermatogonial cells, and these then grow post-mitotically for ~4 days in preparation for meiosis and sperm differentiation [White-Cooper 2010]. In whole unfixed testes, fluorescent protein from a control *His2AVDendra2* gene (a histone variant gene located outside of the histone locus with introns and conventional 3' transcript processing) labels the nuclei of all germline and somatic cells (**Supplementary Figure 1a, Figure 4a**), consistent with its ubiquitous expression and deposition into chromatin. In contrast, fluorescent protein from the *His3Dendra2* HRU is undetectable throughout the interior germline portion of the testes, and only the nuclei of the somatic sheath cells encasing the germline show fluorescent signal (**Supplementary Figure 1b, Figure 4b**). Finally, the apical portion of the testes of the *His2ADendra2* HRU show no fluorescence, but differentiating germline cells display fluorescence once they become most-mitotic primary spermatocytes (**Supplementary Figure 1c, Figure 4c**). We attribute this difference between H2A-Dendra2 and H3Dendra2 fusion proteins to the ability of histone H2A to deposit onto DNA in post-mitotic cells, while histone H3 cannot [MacAlpine & Almouzni 2013]. This implies that the HRU is most strongly silenced in the germline stem cells and gonial cells in the male germline.

To test if HRU silencing is also sensitive to histone gene dosage in the male germline, we constructed flies deleted for the histone locus, rescued with the 12XWT HRU array, and carrying the *His2ADendra2* reporter HRU. Testes from these flies show intense fluorescence of both apical germline cells and of primary spermatocytes (**Supplementary Figure 1d, Figure 4d**). Thus, we infer that germline cells – like somatic cells – upregulate histone gene expression when their numbers are limiting.

Excess histone H4 silences histone genes

Histones are essential for cell proliferation and viability, but males can survive with defects in the germline. Thus, we examined the effects of targeted RNAi knockdown on HRU silencing in the male germline. We expected that knockdown of a silencing component would derepress histone-Dendra2 HRU reporters, and so we screened a set of inducible RNAi constructs where small RNA is specifically produced in the gonial cells of adult testis (**Supplementary Table 2**). We targeted the enzymes that catalyze the marks enriched at the histone locus in somatic wing disc cells (**Table 1**). Knockdown of the histone H3 lysine-9 methyltransferase *eggless* (*egg* [Clough et al 2007]) did not derepress HRU reporters, nor did knockdown of the H3K-9me2/3-binding protein HP1 [James et al 1989] or HP2 [Shaffer et al 2002]. Knockdown of the histone H2A ubiquitin ligase *Sex combs extra* (*Sce* [Gutierrez et al 2012]), the PRC1 component *Polycomb* (*Pc* [Lanzuolo & Orlando 2012]), or the histone H3 lysine-27 methyltransferase *Enhancer of zeste* (*E(z)* [Cao & Zhang 2004]) did not affect HRU silencing.

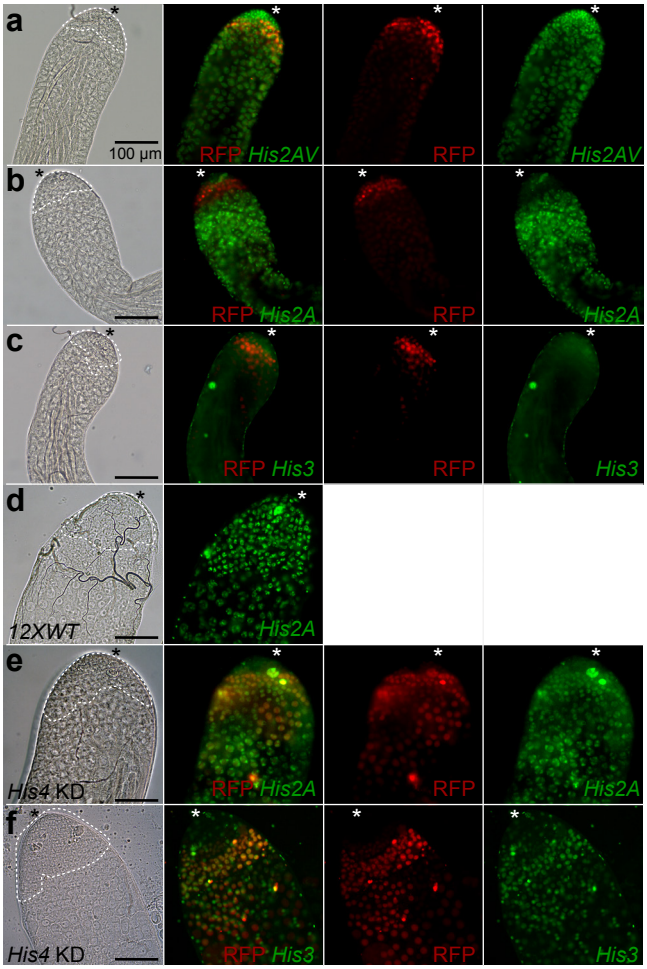

Figure 4. Silencing and derepression of reporter HRUs in the male germline. Gonial cells in the testis apical tip are marked by *bamGAL4*-induced *UASRFP* expression (red). The zone containing germline stem cells and spermatogonial cells are outlined with white dashed lines on phase contrast images. **(a)** Fluorescence of *His2AV-Dendra2* in wildtype males. Staining is apparent in the apical tip of the testis, in gonial cells, and in post-mitotic germline stages. **(b)** Fluorescence of the *His2ADendra2* HRU reporter in wildtype males. Staining is absent in the apical tip of the testis and in gonial cells, but is present in post-mitotic germline stages. **(c)** Fluorescence of the *His3Dendra2* HRU reporter in wildtype males. Staining is absent throughout the germline, the few fluorescent nuclei are in somatic cells of the testis sheath. **(d)** Fluorescence of the *His2ADendra2* HRU reporter in 12XWT males. This line does not carry the *bamGAL4* and *UAS-RFP* constructs, and germline stem cells and gonial cells were identified by nuclear morphology and position in the testis (dashed line). Strong H2ADendra2 fluorescence is apparent in the apical tip of the testis, in gonial cells, and in post-mitotic germline stages. **(e)** Fluorescence of the *His2ADendra2* HRU reporter in males with *bamGAL4*-induced knockdown (KD) of *His4*. Staining is absent in the apical tip of the testis, but appears in gonial cells and in post-mitotic germline stages. **(f)** Fluorescence of the *His3Dendra2* HRU reporter in males with *bamGAL4*-induced knockdown (KD) of *His4*. Staining is absent in the apical tip of the testis, but appears in gonial cells and in post-mitotic germline stages.

Previous work has implicated the H3K9-methyltransferase *Suppressor of variegation 3-9* (*Su(var)3-9*) in histone gene silencing [Ner et al 2002; Ito et al 2012], and indeed we find that the histone locus is enriched for H3K9 methylation (**Figure 2**). Publicly available RNAi constructs targeting the main H3K9-methyltransferase *Suppressor of variegation 3-9* (*Su(var)3-9*) cross-react to the overlapping essential gene for the eIF2 translation factor (and this co-knockdown eliminates the male germline; **Supplementary Table 2**), preventing knockdown tests in the germline. Instead, we constructed viable null *Su(var)3-9* flies from transheterozygous point mutation alleles [Schotta et al 2002]. Neither *His2A-Dendra2* nor *His3Dendra2* reporters are derepressed in this null background (**Supplementary Table 2**). Thus, it appears that while silenced HRUs carry modifications associated with heterochromatic silencing, these modifications do not control histone gene expression to the extent that changes in gene number does.

To determine if levels of histone proteins alter HRU silencing, we used RNAi constructs targeting each of the core histone genes *His3*, *His4*, *His2A*, and *His2B*, and to the linker histone *His1* in gonial cells of the male germline. We also tested constructs targeting the histone variant genes for *His2AV*, *His3.3A*, and *His3.3B*, as well as the orphan gene *His4R*. Of these nine genes, only knockdown of *His4* affects HRU silencing, resulting in dramatic derepression of *His2ADendra2* and of *His3Dendra2* in gonial cells (**Supplementary Table 2**, **Figure 4e,f**). Expression of these reporters is absent in germline stem cells, where the RNAi construct is not yet induced.

It is surprising that levels of only one histone modulate HRU silencing, since histones associate in dimers and in octamers as nucleosomes are assembled. We therefore examined the localization of different histones within the male germline, using inducible GFP-tagged constructs [Schwartz & Ahmad 2005; **Methods**]. Induction of a tagged histone H3 in gonial cells labels the nuclei of these mitotically-active cells, as does induced expression of tagged H3.3 (**Figure 5a,b**). Induced GFP-tagged histone H4 also labeled the chromatin of gonial cells (**Figure 5c**), but with a subnuclear pattern distinct from the other histones (**Figure 5d**); nuclei with H4-GFP show one large dot of the tagged protein over a widespread background. This H4-GFP dot coincides with Mxc protein at the HLB in gonial cells (**Figure 5e**),

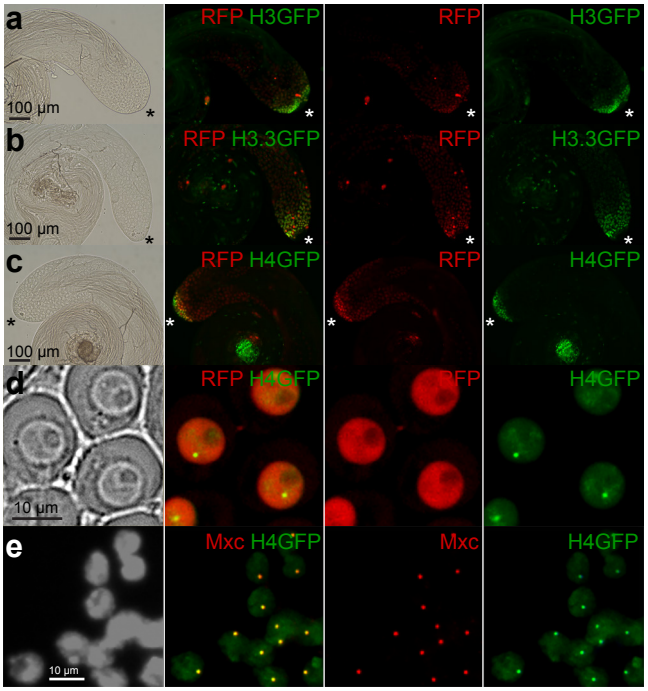

Figure 5. Histone H4 is a component of the Histone Locus Body in male germline cells. Gonial cells in the testis apical tip are marked by *bamGAL4*-induced *UASRFP* expression (red). **(a)** Expression of *bamGAL4*-induced histone H3-GFP in gonial cells of the male germline. **(b)** Expression of *bamGAL4*-induced histone H3.3-GFP in gonial cells of the male germline. **(c)** Expression of *bamGAL4*-induced histone H4-GFP in gonial cells of the male germline. **(d)** Subnuclear localization of *bamGAL4*-induced histone H4-GFP in RFP-labeled gonial cells. H4-GFP broadly stains the nucleus, and forms one intense dot in each nucleus. **(e)** The *bamGAL4*-induced histone H4-GFP in gonial cells coincides with the Mxc protein in the HLB.

suggesting a direct role in histone gene expression.

To define the dynamics of histone H4 localization to the HLB in the male germline, we immunostained fixed testes with antibodies to various components of the HLB. Mxc is a constitutive component of the HLB in somatic cells [White et al 2011]; it is also present in the nuclei of germline gonial cells (**Figure 6a**). In the mitotically active cells at the apical tip of the testes anti-Mxc antibodies label a single large HLB. Slightly later in spermatogenesis in primary spermatocytes, the HLB is divided into 2-4 smaller dots (**Supplementary Figure 2**), consistent with the unpairing of homologous loci in this post-mitotic stage [Vazquez et al 2002]. Mxc then disappears from nuclei in the mid-primary spermatocyte stage. Mxc is phosphorylated by cyclin E/Cdk2 kinase in S phase of the cell cycle [White et al 2007], and this phospho-epitope is recognized by the MPM2 antibody [Davis et al 1983]. Indeed, MPM2 antibody stains foci that colocalize with Mxc in the very apical tip of the testis, marking the mitotically active cells (**Figure 6a**). In slightly later stages MPM2 signal at the HLB diminishes, and new staining appears in the nucleolus and nucleoplasm in primary spermatocytes (**Supplementary Figure 2,** [Okazaki et al 2020]), which we attribute to other protein targets of the MPM2 antibody.

Staining testes with induced histone H4-GFP with anti-MPM2 antibody revealed that the H4 dot is most intense in spermatogonial cells immediately after mitosis (**Figure 6b,c**): cells with the most intense H4-GFP signal are immediately distal to the mitotic zone with reduced MPM2 signal, compared to more apical cells. As anticipated from chromatin profiling (**Figure 1**) and from published work in the female germline [Lu et al 2024], the HLB in male gonial cells is the major site of RNAPII-S5p in the nucleus (**Figure 6d,e**). This RNAPII-S5p dot colocalizes with Mxc and MPM2 throughout the apical tip of the testis, so this must be the major RNAPII isoform when the histone genes are being transcribed in S phase cells. The HLB continues to be enriched for RNAPII-S5p in slightly older gonial cells with H4GFP signal, but is reduced in the HLB by the early primary spermatocyte stage (**Figure 6d**), indicating shutdown of the HLB as germline cells differentiate. In contrast, the RNAPII-S2p isoform is broadly present throughout the nucleus in all germline cells with no greater enrichment in the HLB than other chromatin (**Figure 6f**). Using an antibody to histone H4, a weak H4 dot is also visible in 94% (47/50) of germline cells undergoing S phase but only 7% (1/14) of mitotic cells (**Figure 6g-i**). This reduction at mitosis coincides with the partial disassembly of the HLB at this time [White et al 2011]. Low H4 staining in cycling spermatogonial cells and higher staining in post-mitotic cells suggests that histone H4 marks silenced histone gene copies in the active HLB and when the HLB is shut down.

Human histone H4 genes are hyper-enriched for the NPAT transcription factor and RNAPII

HLBs are nuclear features in human cells, and are marked by the Mxc homolog NPAT [Ma et al 2000]. Staining of human K562 nuclei with antibodies to NPAT and to histone H4 reveals that histone H4 is a conserved component of HLBs in animal cells (**Figure 7a**). In the human genome the multicopy histone genes are clustered but with more spacing between genes than in the repetitive array in Drosophila [Amatori et al 2021]. To distinguish binding between active and silent histone genes, we examined our previously published profiling data of NPAT and RNAPII in K562 cell lines [Kaya-Okur et al 2019, Janssens et al 2021]. Strikingly, NPAT binds at some but not all replication-dependent histone genes, and each NPAT-bound histone gene is expressed, while histone genes without NPAT have

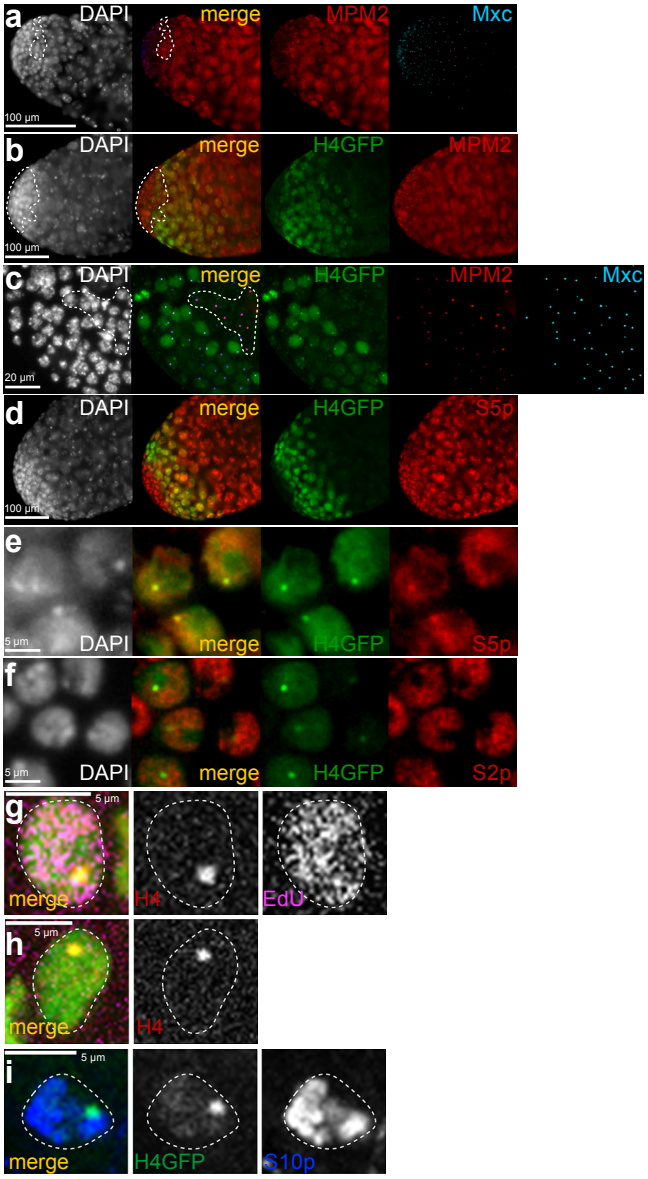

Figure 6. Histone H4 is enriched in the inactive Histone Locus Body of spermatogonial cells. Imaging of the apical tip of the testis. Dashed lines indicate the mitotic zone defined by high MPM2 staining. **(a)** A major focus of RNAPII-S5p coincides with the active HLB marked by Mxc and MPM-2. **(b)** The RNAPII-S2p isoform is broadly distributed in gonial cell nuclei but not enriched in the HLB. **(c,d)** Gonial cell nuclei with bright dots of *bam-GAL4*-induced H4-GFP have relatively weak MPM-2 staining, and lie slightly distal to gonial cells with bright MPM2 staining in the testis. **(e,f)** *bamGAL4*-induced H4-GFP coincides with the major focus of RNAPII-S5p in gonial cells. **(f,g)** Representative spermatogonial cell labeled with EdU to mark nuclei with ongoing DNA replication. The H4 dot is present in both S-phase and G2-phase cells. **(h)** Representative spermatogonial cell marked with the M-phase epitope H3S10p. The H4 dot is visible in only some germ cells in prophase.

less polymerase (**Figure 7b,c**). Profiling of histone H4 reveals that the majority of signal falls at the histone clusters, and precisely coincides with NPAT at histone gene promoters (**Figure 7b,c; Supplementary Figure 3**). While NPAT is found at the promoters of all histone subtypes, it is highly significantly enriched at the promoters of histone H4 genes (**Figure 7d**). These histone H4 genes are more highly expressed than the genes for its partner histone H3, suggesting that excess amounts of histone H4 are produced in cells.

Discussion

The histone genes in Drosophila not only respond to cell proliferation signals, but also are also subject to heterochromatic silencing due to their repetitive sequence arrangement. Our results infer that the normal state of the repetitive wildtype histone locus is a mixture of transcriptionally activated histone genes with active histone marks and silenced histone genes with repressive marks. This parallels the functional organization of ribosomal RNA genes, where actively transcribed units are intermixed with silenced units with concordant chromatin markings [Grummt & Pikaard 2003]. In both cases a mixture of active and silenced genes may allow cells to fine-tune histone production to the needs of cell proliferation and growth, the rates of which vary between tissues and life stages. Our results indicate that the predominant mechanism of regulating the histone genes is in response to the demand for chromatin packaging in proliferating cells. This includes both the activation of more genes, as well as increasing the number of RNAPII molecules loading on each gene.

How might cells sense the need for more histones? Our observations suggest a simple model, where soluble histone H4 protein directly represses histone gene transcription. In this way, ongoing DNA replication and chromatin packaging would use up soluble histones, including histone H4, leading to activation of histone genes and more histone synthesis. Once DNA replication ceases, soluble histones accumulate, histone H4 localizes to the HLB, and then represses transcription. The conserved localization of histone H4 to the HLB of K562 cells suggests that this mechanism may also operate in humans. While histone H4 normally dimerizes with a partner histone, small amounts of monomeric histone complexed with protein chaperones have been observed [Apta-Smith et al 2018]. There are analogous instances where a singular histone is used to measure chromatin needs: in early Drosophila syncytial embryos soluble maternal histone H3 protein inhibits the Chk1 cyclin kinase; as soluble pools of this histone are depleted kinase inhibition is relieved and introduces gap phases into late embryo cell cycles [Shindo &

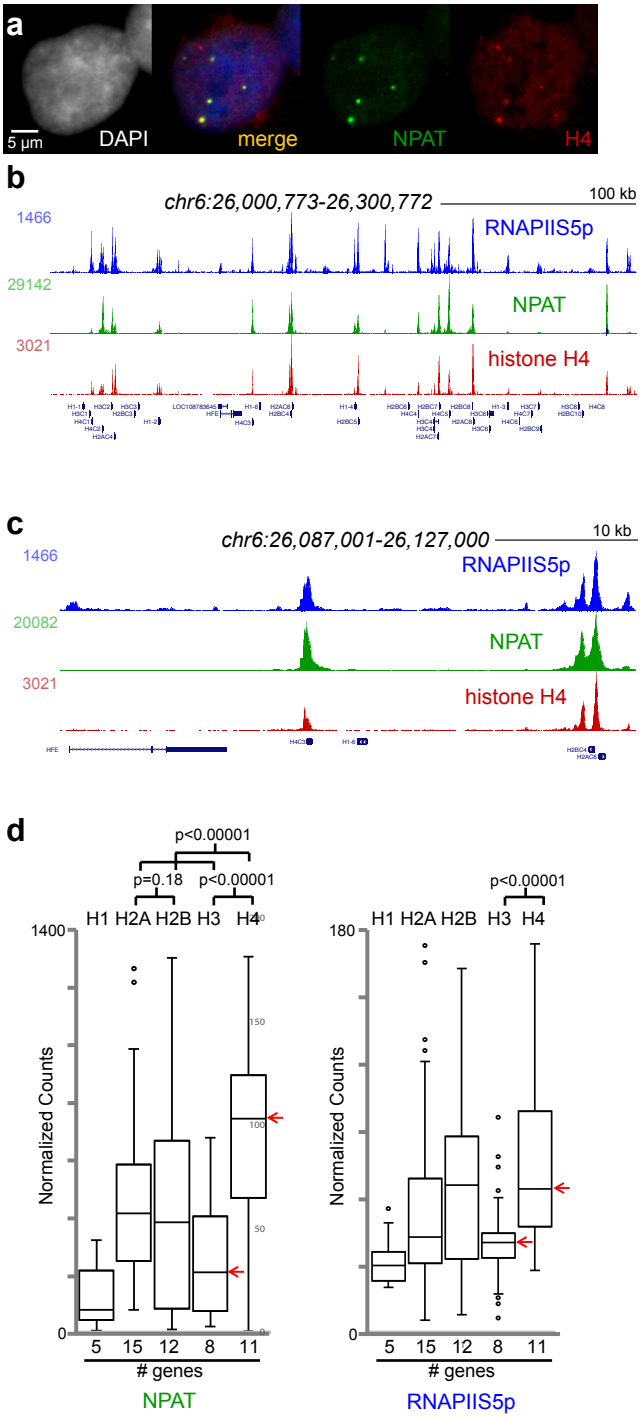

Figure 7. NPAT binding at active histone genes in human K562 cells. (a) Browser tracks of NPAT and RNAPII across portions of the HIST1 histone cluster. Blue shading marks histone H4 genes. **(b)** Distributions of NPAT and RNAPII signal at each histone subtype gene. Medians and S.E. intervals are indicated in boxplots, and the difference in medians between H3 and H4 histone subtypes is marked in red. **(c)** Localization of anti-histone H4 signal to the multiple HLBs in a K562 nucleus.

Amodeo 2021]. Thus, this soluble histone singlehandedly measures the number of nuclei in the embryo, and coordinates cell cycle behavior with the nuclear-to-cytoplasmic ratio. In human cells, histone H2B binds to extrachromosomal DNA such as that of DNA viruses, and serves as a binding platform for the Interferon-beta Promoter Stimulator-1 factor that stimulates apoptosis of infected cells [Kobiyama et al 2010]. These instances fit with a general biological strategy of sensing the amount of DNA in a cell using one essential component of chromatin packaging.

It is intriguing that the human histone gene regulatory factor NPAT predominantly binds the promoters of histone H4 genes. The NPAT homolog Mxc in Drosophila is crucial for seeding the aggregation of the HLB and for stimulating transcription of histone genes therein [Hur et al 2020]. If these functions are conserved, the implication is that active histone H4 gene promoters nucleate the formation of the HLB in human cells and dictate which clusters of histone genes can be active and which clusters may degrade to pseudogenes.

Chromatin packaging with histones is a universal feature of eukaryotes, but a clear picture of their ancient evolutionary origins has only accrued recently. Phylogenetic evidence places the histone H4s as a sister lineage to both the HMfB archaeal histones and the doublet H4-H3 histones of the Nucleocytoviricota giant viruses [Grau-Bové et al 2022], which diversified into the four core histone subtypes in the last common ancestor of eukaryotes [Malik and Henikoff 2003]. The stem-loop structure of core histone mRNAs in animals and the ancestral stem-loop binding protein (SLBP) that directs 3' processing of transcripts closely parallels the 3' stem-loop/NusA transcription termination machinery in bacteria [Shine et al 2024], and the co-occurrence and loss of both the stem-loop and SLBP places the origin of histone mRNA 3' processing at the base of the eukaryotic tree [Lopez & Samuelsson 2008]. It is so conceivable that histone H4 has been used as a negative regulator of core histone gene expression since the origin of eukaryotic histones.

Most core histones have evolved specialized subtypes, but histone H4 is distinctive in that very few variants occur across eukaryotic evolution. One exception occurs in the bracoviruses, which encode a histone H4 variant that is distinguished from the ancestral H4 by a 38 aa N-terminal extension. Parasitic braconid wasps harboring an endogenous bracovirus inject DNA encoding viral H4 into host moth larvae, resulting in production of this variant histone and suppression of host histone H4 mRNA production [Gad & Kim 2009]. This well-conserved phenomenon in which an unaccompanied H4 histone causes repression parallels the negative feedback loop we infer for suppression of the HLB more generally.

Methods

Fly strains

All crosses were performed at 25˚C. All mutations and chromosomal rearrangements used here are described in Flybase (http://www.flybase.org). The *w*^{1118} strain was used as a wildtype control. The *12XWT* strain is *w ; DHis*^{C} *; 12XWT* [MacKay et al 2015]. The HRU reporter *His3Dendra2* was previously described [Shindo & Amodeo 2019], and the *His2ADendra2* reporter was constructed similarly. Inducible histone lines were *UAS-H3-GFP* [Schwartz & Ahmad 2005], *UAS-H3.3-GFP* [Schwartz & Ahmad 2005], and the *UAS-H4-GFP* construct [Ahmad & Henikoff 2002] was injected into fly embryos for P element transformation [Rubin & Spradling 1982] by BestGene Inc. (Chino Hills CA). A similar UAS-H4-eGFP construct used here for some experiments was previously published [Wooten et al 2019]. Additional constructs used for cytological characterization were *y w P[bam-GAL4:VP16,w*$^{+}$*]1/Y ; P[UAS-RFP,w*$^{+}$*]2*. Inducible knockdown constructs and Bloomington Drosophila Stock Center IDs for histones and chromatin regulators are listed in the *Key Resources Table*.

Antibodies

Antibodies used for CUT&Tag profiling and for immunocytology are listed in the *Key Resources Table*.

Imaging unfixed tissues

Dissected tissues from larvae or adults were mounted in PBS on slide and imaged by epifluorescence on an EVOS FL Auto 2 inverted microscope (Thermo Fisher Scientific) with a 10X, 20X, or 40X objective. Pseudo-colored images were adjusted and composited in Adobe Photoshop and Adobe Illustrator.

Imaging immunostained testes

Testes from one-day old adult males were dissected and fixed in 4% formaldehyde/PBS with 0.1% Triton-X100 (PBST) for 10 minutes, incubated in 0.3% sodium deoxycholate/PBST 2X for 10 minutes each [Lim & Fuller 2012], and then incubated with primary antibodies in A+t buffer at 4˚C overnight and then with fluorescently-labeled secondary antibodies (1:200 dilution, Jackson ImmunoResearch). Testes were stained with 0.5 µg/mL DAPI/PBS and mounted in 80% glycerol on slides, and imaged by epifluorescence on an EVOS FL Auto 2 inverted microscope (Thermo Fisher Scientific) with a 10X or with a 40X objective. Pseudo-colored images were adjusted and composited in Adobe Photoshop and Adobe Illustrator.

Imaging spermatocytes

Testes from third-instar male larvae were prepared as described [Bonaccorsi et al 2000]. Briefly, one testis was dissected in a drop of PBS on a Histobond glass slide (VWR 16004-406), squashed gently with a RainX (ITW Global Brands) coated coverslip, then flash-frozen in liquid nitrogen. After popping off the coverslip, the sample was fixed with 4% formaldehyde/PBST for 5 minutes, and incubated with 0.3% sodium deoxycholate/PBST twice for 10 minutes each. Samples were incubated with primary antiserum in A+t buffer, and finally with fluorescently-labeled secondary antibodies (1:200 dilution, Jackson ImmunoResearch). Slides were stained with 0.5 µg/mL DAPI/PBS, mounted in 80% glycerol, and imaged by epifluorescence on an EVOS FL Auto 2 inverted microscope (Thermo Fisher Scientific) with a 40X objective. Pseudo-colored images were adjusted and composited in Adobe Photoshop and Adobe Illustrator.

Imaging human K562 cells

K562 cells were swelled with a hypotonic 0.5% sodium citrate solution, then smashed onto glass slides in a Cytospin 4 centrifuge (Thermo). Slides were fixed with 4% formaldehyde/PBST and incubated with primary antisera in A+t buffer, then with fluorescently-labeled secondary antibodies (1:200 dilution, Jackson ImmunoResearch), stained with 0.5 µg/mL DAPI/PBS, mounted in 80% glycerol, and imaged by epifluorescence on an EVOS FL Auto 2 inverted microscope (Thermo Fisher Scientific) with a 40X objective. Pseudo-colored images were adjusted and composited in Adobe Photoshop and Adobe Illustrator.

Chromatin profiling

To perform CUT&Tag [Kaya-Okur et al 2019], we dissected 20 imaginal wing discs from male 3rd instar larvae in PBS buffer, and transferred them to a tube containing Accutase (Stemcell Technologies, #07920) at 25˚C for 30 minutes. We then added an equal volume of 30% BSA to block proteases, and ran the material through a 30 ½ gauge needle once to dissociate tissue. Tissue suspensions were divided between 4-8 reaction tubes, and bound with BioMag Plus ConA (Bangs Inc., #531) magnetic beads, and then incubated with the following CUT&Tag solutions sequentially: primary antibodies diluted in Wash+ buffer (20 mM HEPES pH 7.5, 150 mM NaCl, 0.5 mM spermidine, 0.05% triton-X100, 2 mM EDTA, 1% BSA, with Roche cOmplete protease inhibitor) overnight at 4˚, secondary antibodies (in Wash+ buffer) for 1 hour at room temperature, and then incubated with pAGTn5 (Epicypher 15-1017) in 300Wash+ buffer (20 mM HEPES pH 7.5, 300 mM NaCl, 0.5 mM spermidine, 0.05% triton-X100 with cOmplete protease inhibitor) for 1 hour. After one wash with 300Wash+ buffer, samples were incubated in 300Wash+ buffer supplemented with 10 mM $MgCl_2$ for 1 hour at 25˚C to tagment chromatin. Samples were

washed with 10 mM TAPS pH 8.5 and DNA was released with 0.1% SDS, 0.012 U/µL thermolabile protease K (NEB P8111S) in 10 mM TAPS at 37˚ and inactivated at 55˚C. For profiling histone H4 in K562 cells, the same procedure was followed, but cells were fixed onto magnetic beads with 1% formaldehyde for 10 minutes at 25˚C before antibody incubation, and tagmented with a low-salt CUTAC buffer (10 mM TAPS, 5 mM $MgCl_2$, 20% DMF, 0.05% Triton-X100) [Henikoff et al 2020]. Libraries were enriched with 14 cycles of PCR as described [Kaya-Okur et al 2019], and sequenced in dual-indexed paired-end mode (PE50) on the Illumina NextSeq 2000 platform at the Fred Hutchinson Cancer Center Genomics Shared Resource. Paired-end reads were mapped to this assembly using Bowtie2 using parameters, e.g.: --end-to-end --very-sensitive --no-mixed --no-discordant -q --phred33 -I 10 -X 700.

Gene score tables

To summarize the enrichment of profiling features across histones, we counted mapped reads from the start to the end of each gene in .bam files using subreads/feature_counts with option '_o'. Counts for each replication-coupled histone were summed, and counts for all genes were scaled by total mapped reads to give Counts per Million (CPM) reads. These values are provided in **Supplementary Table 3**.

Genomic display

Files of mapped reads were converted to genome coverage with bedtools/bamcoverage [Quinlan & Hall 2010] and displayed in the UCSC genome browser [Kent et al 2002]. Selected regions were exported as PDFs and formatted with Adobe Illustrator.

Data availability

Sequencing data have been deposited in GEO under accession code GSE280833.

Acknowledgements

We thank Amanda Amodeo and Yuki Shindo for histone-Dendra2 reporter lines including two unpublished lines: the *His2ADendra2* HRU reporter and the *His2AVDendra2* reporter, Bob Duronio for histone locus rescue lines, Christine Codomo and Jorja Henikoff for technical and bioinformatic support, and Paul Talbert for pointing out the significance of viral histone H4 protein.

Author contributions

K.A. and S.H. conceived the study. K.A., M.W., B.N.T., and V.V. performed the experiments. K.A., S.H., and V.V. performed data analysis. K.A. wrote the manuscript. K.A., S.H., and X.C. reviewed and edited the manuscript. All authors approved the manuscript.

Competing interests

S.H. and K.A. have filed patent applications on related work.

References

Ahmad, K. and S. Henikoff (2002). "The histone variant H3.3 marks active chromatin by replication-independent nucleosome assembly." Mol Cell9(6):1191-200.

Amatori S, Tavolaro S, Gambardella S and Fanelli M. (2021). The dark side of histones: genomic organization and role of oncohistones in cancer. Clin Epigenetics 13(1):71. PMID: 33827674

Apta-Smith, M. J., J. R. Hernandez-Fernaud and A. J. Bowman (2018). "Evidence for the nuclear import of histones H3.1 and H4 as monomers." Embo j 37(19). PMC6166134

Barbour, H., S. Daou, M. Hendzel and E. B. Affar (2020). "Polycomb group-mediated histone H2A monoubiquitination in epigenome regulation and nuclear processes." Nat Commun 11(1): 5947. PMC7683540

Barth, T. K. and A. Imhof (2010). "Fast signals and slow marks: the dynamics of histone modifications." Trends Biochem Sci 35(11): 618-626.

Bonaccorsi, S., C. Pisano, F. Puoti and M. Gatti (1988). "Y chromosome loops in Drosophila melanogaster." Genetics 120(4): 1015-1034. PMC1203565

Bulchand, S., S. D. Menon, S. E. George and W. Chia (2010). "Muscle wasted: a novel component of the Drosophila histone locus body required for muscle integrity." J Cell Sci 123(Pt 16): 2697-2707.

Cao, R., L. Wang, H. Wang, L. Xia, H. Erdjument-Bromage, P. Tempst, R. S. Jones and Y. Zhang (2002). "Role of histone H3 lysine 27 methylation in Polycomb-group silencing." Science 298(5595): 1039-1043.

Cao, R. and Y. Zhang (2004). "The functions of E(Z)/EZH2-mediated methylation of lysine 27 in histone H3." Curr Opin Genet Dev 14(2): 155-164.

Clough, E., W. Moon, S. Wang, K. Smith and T. Hazelrigg (2007). "Histone methylation is required for oogenesis in Drosophila." Development 134(1): 157-165.

Crain, A. T., M. Nevil, M. P. Leatham-Jensen, K. B. Reeves, A. G. Matera, D. J. McKay and R. J. Duronio (2024). "Redesigning the Drosophila histone gene cluster: an improved genetic platform for spatiotemporal manipulation of histone function." Genetics 228(1). PMC11373521

Dávila López M, Samuelsson T. (2008). Early evolution of histone mRNA 3› end processing. RNA 14(1):1-10.

PMID: 17998288

Davis, F. M., T. Y. Tsao, S. K. Fowler and P. N. Rao (1983). “Monoclonal antibodies to mitotic cells.” Proc Natl Acad Sci U S A 80(10): 2926-2930. PMC393946

Duronio, R. J. and W. F. Marzluff (2017). “Coordinating cell cycle-regulated histone gene expression through assembly and function of the Histone Locus Body.” RNA Biol 14(6): 726-738. PMC5519241

Ebert, A., S. Lein, G. Schotta and G. Reuter (2006). “Histone modification and the control of heterochromatic gene silencing in Drosophila.” Chromosome Res 14(4): 377-392.

Elgin, S. C. (1996). “Heterochromatin and gene regulation in Drosophila.” Curr Opin Genet Dev 6(2): 193-202.

Gad W and Kim Y. (2009). N-terminal tail of a viral histone H4 encoded in Cotesia plutellae bracovirus is essential to suppress gene expression of host histone H4. Insect Mol Biol. 18(1):111-8. PMID: 19196351

Grau-Bové X, Navarrete C, Chiva C, Pribasnig T, Antó M, Torruella G, Galindo LJ, Lang BF, Moreira D, López-Garcia P, Ruiz-Trillo I, Schleper C, Sabidó E, and Sebé-Pedrós A. (2022). “A phylogenetic and proteomic reconstruction of eukaryotic chromatin evolution.” Nat Ecol Evol. 6(7):1007-1023. PMID: 35680998

Grummt, I. and C. S. Pikaard (2003). “Epigenetic silencing of RNA polymerase I transcription.” Nat Rev Mol Cell Biol 4(8): 641-649.

Günesdogan, U., H. Jäckle and A. Herzig (2010). “A genetic system to assess in vivo the functions of histones and histone modifications in higher eukaryotes.” EMBO Rep 11(10): 772-776. PMC2948182

Gutiérrez, L., K. Oktaba, J. C. Scheuermann, M. C. Gambetta, N. Ly-Hartig and J. Müller (2012). “The role of the histone H2A ubiquitinase Sce in Polycomb repression.” Development 139(1): 117-127. PMC3253035

Henikoff, S., J. G. Henikoff, H. S. Kaya-Okur, and K. Ahmad (2020). “Efficient chromatin accessibility mapping in situ by nucleosome-tethered tagmentation.” eLife 9:e63274. PMC7721439

Huang, S.-K., P. H. Whitney, S. Dutta, S. Y. Shvartsman, C. A. Rushlow (2021). “Spatial organization of transcribing loci during early genome activation in Drosophila.” Current Biology 31(22):5102-5110. PMC8612988

Hur W, Kemp JP Jr, Tarzia M, Deneke VE, Marzluff WF, Duronio RJ and Di Talia S. (2020). CDK-Regulated Phase Separation Seeded by Histone Genes Ensures Precise Growth and Function of Histone Locus Bodies. Dev Cell 54(3):379-394. PMID: 32579968

Ito, S., S. Fujiyama-Nakamura, S. Kimura, J. Lim, Y. Kamoshida, Y. Shiozaki-Sato, S. Sawatsubashi, E. Suzuki, M. Tanabe, T. Ueda, T. Murata, H. Kato, F. Ohtake, R. Fujiki, T. Miki, A. Kouzmenko, K. Takeyama and S. Kato (2012). “Epigenetic silencing of core histone genes by HERS in Drosophila.” Mol Cell 45(4): 494-504.

James, T. C., J. C. Eissenberg, C. Craig, V. Dietrich, A. Hobson and S. C. Elgin (1989). “Distribution patterns of HP1, a heterochromatin-associated nonhistone chromosomal protein of Drosophila.” Eur J Cell Biol 50(1): 170-180.

Janssens, D.H., Meers, M.P. Wu, S.J., Babaeva, E., Meshinchi, S., Sarthy, J.F., Ahmad, K., and Henikoff, S. (2021). “Automated CUT&Tag profiling of chromatin heterogeneity in mixed-lineage leukemia.” Nat Genet. 53(11):1586-1596. PMID: 34663924

Kaya-Okur, H. S., S. J. Wu, C. A. Codomo, E. S. Pledger, T. D. Bryson, J. G. Henikoff, K. Ahmad and S. Henikoff (2019). “CUT&Tag for efficient epigenomic profiling of small samples and single cells.” Nat Commun 10(1): 1930. PMC6488672

Kent, W. J., C. W. Sugnet, T. S. Furey, K. M. Roskin, T. H. Pringle, A. M. Zahler and D. Haussler (2002). “The human genome browser at UCSC.” Genome Res 12(6): 996-1006. PMC186604

Kobiyama, K., Takeshita, F., Jounai, N., Sakaue-Sawano, A., Miyawaki, A., Ishii, K.J., Kawai, T., Sasaki, S., Hirano, H., Ishii, N., Okuda, K., and Suzuki, K. (2009). “Extrachromosomal histone H2B mediates innate antiviral immune responses induced by intracellular double-stranded DNA.” J Virol. 84(2):822-32. PMID: 19906922

Lanzuolo, C. and V. Orlando (2012). “Memories from the polycomb group proteins.” Annu Rev Genet 46: 561-589.

Lim, J. G. and M. T. Fuller (2012). “Somatic cell lineage is required for differentiation and not maintenance of germline stem cells in Drosophila testes.” Proc Natl Acad Sci U S A 109(45): 18477-18481. PMC3494938

Liu, J. L., C. Murphy, M. Buszczak, S. Clatterbuck, R. Goodman and J. G. Gall (2006). “The Drosophila melanogaster Cajal body.” J Cell Biol 172(6): 875-884. PMC2063731

Lu, F., B. J. Park, R. Fujiwara, J. E. Wilusz, D. S. Gilm-

our, R. Lehmann and T. Lionnet (2024). “Integrator-mediated clustering of poised RNA polymerase II synchronizes histone transcription.” bioRxiv. PMC10592978

Ma, T., B. A. Van Tine, Y. Wei, M. D. Garrett, D. Nelson, P. D. Adams, J. Wang, J. Qin, L. T. Chow, and J. W. Harper (2000). “Cell cycle-regulated phosphorylation of p220(NPAT) by cyclin E/Cdk2 in Cajal bodies promotes histone gene transcription.” Genes & Dev 14(18): 2298-2313. PMC316935

MacAlpine, D. M. and G. Almouzni (2013). “Chromatin and DNA replication.” Cold Spring Harb Perspect Biol 5(8): a010207. PMC3721285

McKay, D. J., S. Klusza, T. J. Penke, M. P. Meers, K. P. Curry, S. L. McDaniel, P. Y. Malek, S. W. Cooper, D. C. Tatomer, J. D. Lieb, B. D. Strahl, R. J. Duronio and A. G. Matera (2015). “Interrogating the function of metazoan histones using engineered gene clusters.” Dev Cell 32(3): 373-386. PMC4385256

Ner, S. S., M. J. Harrington and T. A. Grigliatti (2002). “A role for the Drosophila SU(VAR)3-9 protein in chromatin organization at the histone gene cluster and in suppression of position-effect variegation.” Genetics 162(4): 1763-1774. PMC1462387

Okazaki, R., K. Yamazoe and Y. H. Inoue (2020). “Nuclear Export of Cyclin B Mediated by the Nup62 Complex Is Required for Meiotic Initiation in Drosophila Males.” Cells 9(2). PMC7072204

Quinlan, A. R. and I. M. Hall (2010). “BEDTools: a flexible suite of utilities for comparing genomic features.” Bioinformatics 26(6): 841-842. PMC2832824

Rubin, G. M. and A. C. Spradling (1982). “Genetic transformation of Drosophila with transposable element vectors.” Science 218(4570):348-53.

Salzler, H. R., D. C. Tatomer, P. Y. Malek, S. L. McDaniel, A. N. Orlando, W. F. Marzluff and R. J. Duronio (2013). “A sequence in the Drosophila H3-H4 Promoter triggers histone locus body assembly and biosynthesis of replication-coupled histone mRNAs.” Dev Cell 24(6): 623-634. PMC3613982

Schotta, G., A. Ebert, V. Krauss, A. Fischer, J. Hoffmann, S. Rea, T. Jenuwein, R. Dorn and G. Reuter (2002). “Central role of Drosophila SU(VAR)3-9 in histone H3-K9 methylation and heterochromatic gene silencing.” Embo j 21(5): 1121-1131. PMC125909

Schwartz, B. E. and K. Ahmad (2005). “Transcriptional activation triggers deposition and removal of the histone variant H3.3.” Genes Dev 19(7): 804-814. PMC1074318

Schwartz, S., E. Meshorer and G. Ast (2009). “Chromatin organization marks exon-intron structure.” Nat Struct Mol Biol 16(9): 990-995.

Shaffer, C. D., G. E. Stephens, B. A. Thompson, L. Funches, J. A. Bernat, C. A. Craig and S. C. Elgin (2002). “Heterochromatin protein 2 (HP2), a partner of HP1 in Drosophila heterochromatin.” Proc Natl Acad Sci U S A 99(22): 14332-14337. PMC137884

Shindo, Y. and A. A. Amodeo (2019). “Dynamics of Free and Chromatin-Bound Histone H3 during Early Embryogenesis.” Curr Biol 29(2): 359-366.e354.

Shine M, Gordon J, Schärfen L, Zigackova D, Herzel L and Neugebauer KM. (2024). Co-transcriptional gene regulation in eukaryotes and prokaryotes. Nat Rev Mol Cell Biol. 25(7):534-554. PMID: 38509203

Talbert PB, Armache KJ and Henikoff S. (2022). “Viral histones: pickpocket’s prize or primordial progenitor?” Epigenetics Chromatin 15(1):21. PMID: 35624484

Vazquez, J., A. S. Belmont and J. W. Sedat (2002). “The dynamics of homologous chromosome pairing during male Drosophila meiosis.” Curr Biol 12(17): 1473-1483.

White, A. E., B. D. Burch, X. C. Yang, P. Y. Gasdaska, Z. Dominski, W. F. Marzluff and R. J. Duronio (2011). “Drosophila histone locus bodies form by hierarchical recruitment of components.” J Cell Biol 193(4): 677-694. PMC3166876

White, A. E., M. E. Leslie, B. R. Calvi, W. F. Marzluff and R. J. Duronio (2007). “Developmental and cell cycle regulation of the Drosophila histone locus body.” Mol Biol Cell 18(7): 2491-2502. PMC1924828

White-Cooper, H. (2010). “Molecular mechanisms of gene regulation during Drosophila spermatogenesis.” Reproduction 139(1): 11-21.

Wooten, M., Snedeker, J., Nizami, Z.F., Yang, X., Ranjan, R., Urban, E., Kim, J.M., Gall, J., Xiao, J., and Chen, X. (2019). “Asymmetric histone inheritance via strand-specific incorporation and biased replication fork movement.” Nat Struct Mol Biol. 26(8):732-743. PMID: 31358945

Zhang, W., X. Zhang, Z. Xue, Y. Li, Q. Ma, X. Ren, J. Zhang, S. Yang, L. Yang, M. Wu, M. Ren, R. Xi, Z. Wu, J. L. Liu, E. Matunis, J. Dai and G. Gao (2019). “Probing the Function of Metazoan Histones with a Systematic Library of H3 and H4 Mutants.” Dev Cell 48(3): 406-419.e405. PMC6595499

Supplementary Information

Bioinformatics for figures:

For Figure 1: mapped reads for Mute (BT2579), Mxc (BT3065), Rpb1 (BT542), RNAPII-S5p (BT1781), and RNAPII-S2p (BT3067) were converted to bigwigs with bedtools/genome coverage and displayed in the UCSC genome browser.

For Figure 2: Mapped reads for H3K9me1 (BT1777), H3K9me2 (BT1778), H3K9me3 (BT1175), H3K27me3 (BT1173), uH2A (BT827), H3K4me1 (BT3072), H3K4me2 (BT3068), H3K4me3 (BT3074), H3K27ac (BT3069), and H3K36me3 (BT826) were converted to bigwigs with bedtools/genome coverage and displayed in the UCSC genome browser.

For Figure 7: (b,c) mapped reads for NPAT (SH_Hs_NPB4_20190217), RNAPII (SH_Hs_K5xlin_PolS5P_20k_0320), and histone H4 (BT_Hs_3518) were converted to bedgraph files and displayed in the UCSC genome browser. **(d)** For counting signal at histone gene subtypes, histone genes were scored as active by clear peaks of RNAPII signal, and normalized counts at each of these genes was summed for each histone subtype. 8 replicates for NPAT profiling and 5 replicates of RNAPII profiling were analyzed and tested by Mann-Whitney U-tests. NPAT samples were SH_Hs_NPA1_20190217, SH_Hs_NPA2_20190217, SH_Hs_NPA4_20190217, SH_Hs_NPA8_20190217, SH_Hs_NPB1_20190217, SH_Hs_NPB2_20190217, SH_Hs_NPB4_20190217, and SH_Hs_NPB8_20190217 [Kaya-Okur et al 2019]. RNAPII samples were SH_Hs_K5xlin_PolS5P_3cy_0320, SH_Hs_K5xlin_PolS5P_6cy, SH_Hs_K5xlin_PolS5P_9cy_0320, SH_Hs_K5xlin_PolS5P_12cy_0320, and SH_Hs_K5xlin_PolS5P_20k_0320 [Janssens et al 2021].

For Table 1: Replicate .bam files were counted using subReads/featureCounts with option “-o” across a list of all annotated UCSC knownGenes in the dm6 genome assembly. Reads for each histone subtype were summed for each genotype, and counts in each histone subtype in the 12X line were divided by counts in the wildtype line.

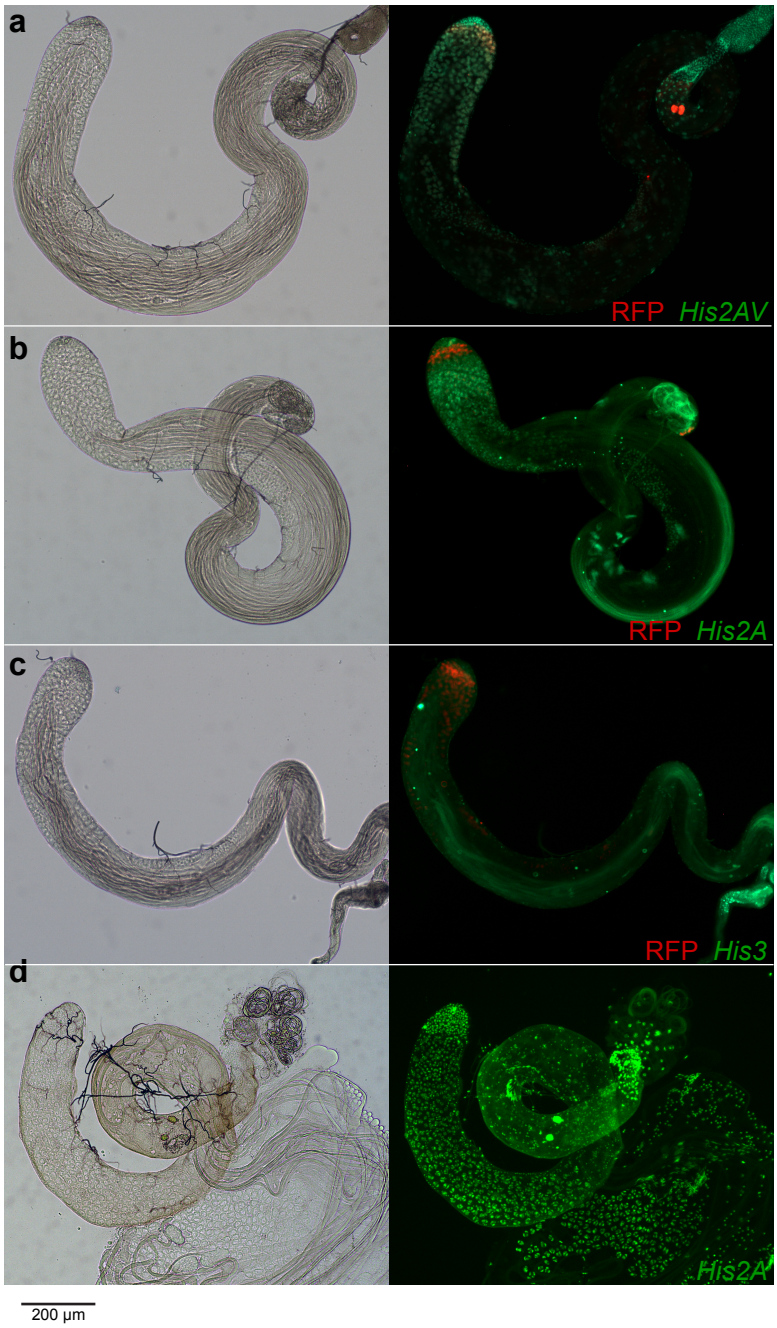

Supplementary Figure 1. Silencing and expression of reporter histones and HRUs in the Drosophila testes. 10X magnification images of entire testes.
(a) Expression of *His2AVDendra2* in wildtype testis.
(b) Expression of *His2ADendra2* HRU in wildtype testis.
(c) Expression of *His3Dendra2* HRU in wildtype testis.
(d) Expression of *His2ADendra2* HRU in the testis of 12XWT males.

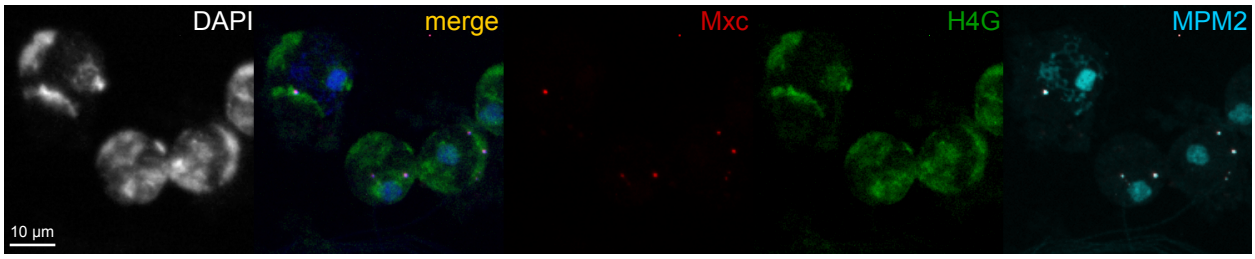

Supplementary Figure 2. Dynamics of the HLB and MPM2 epitopes in the Drosophila male germline. Patterns of Mxc and MPM2 in post-mitotic primary spermatocyte stages. The HLB splits into two dots in each nucleus due to the loss of somatic pairing at this stage. The MPM2 phospho-epitopes stains the HLB at a low level in primary spermatocytes, but also stains the nucleolus and spermatocyte chromosome loops in slightly later stages.

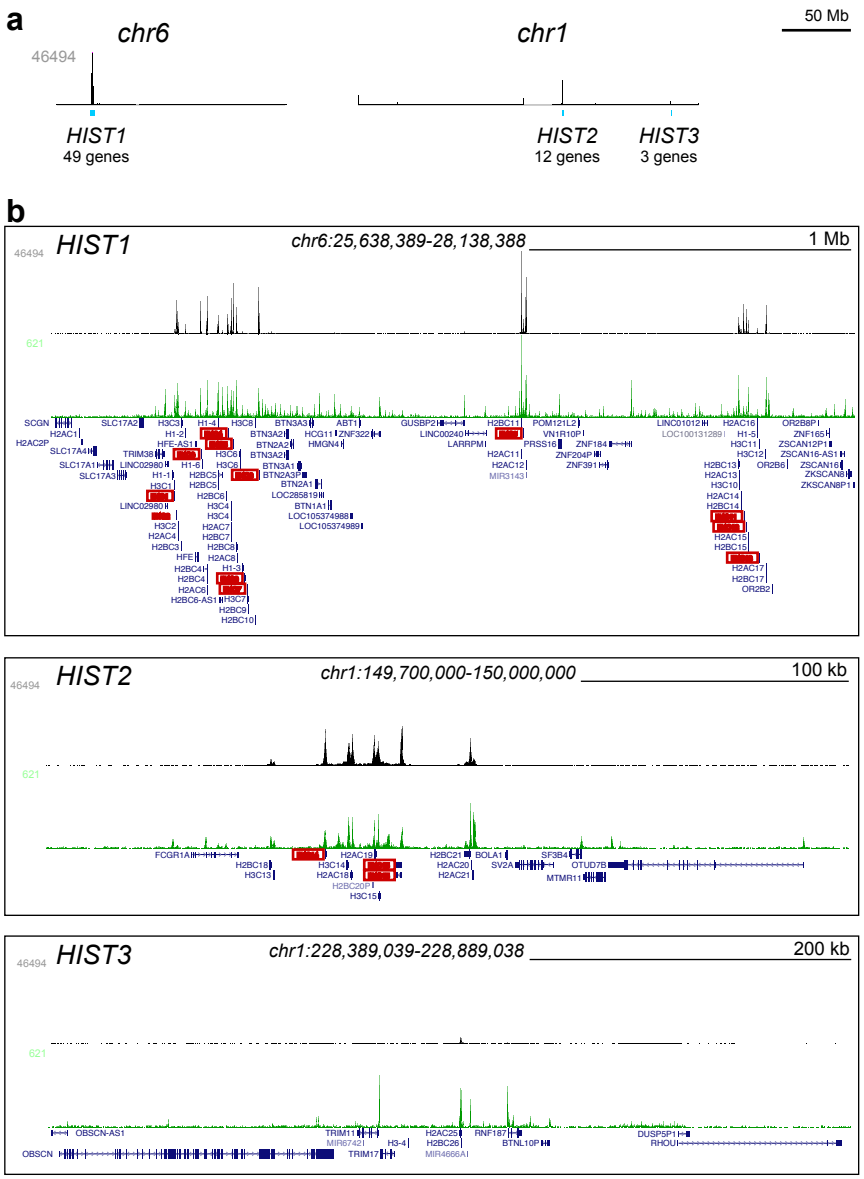

Supplementary Figure 3. Enrichment of NPAT and RNAPII across the Histone gene clusters in human K562 cells.

(a) NPAT signal (black) across chromosomes *6*, *1* and *X* in the hg19 assembly. Blue bars mark the location of the three major Histone clusters, with the number of histone genes indicated.

(b) NPAT (black) and RNAPIIS5p (green) signal across three HIST clusters. Histone H4 genes are marked in red.

Supplementary Table 1. Sample IDs and sequencing results.
Attached spreadsheet.

Supplementary Table 2. Effects of RNAi knockdowns and mutations on HRU reporter expression in the male germline.

		***HRU* expression**	
Mutations	**line[a]**	***His2ADendra2*[b]**	***His3Dendra2*[c]**
none (control)	*w*^{1118}		
HisC deletion and rescue	*ΔHisC; 12XWT/+*		n.d.
Su(var)3-9 null	*Su(var)3-9*^{1}*/Su(var)3-9*^{2}		
RNAi targets			
Su(var)3-9	33401	no germline	no germline
Su(var)3-9	43661	no germline	no germline
egg	34803		
egg	36797		
E(z)	33659		
Sce	35446		
Sce	61312		
HP1	33400		
HP1	36792		
HP2	38255		
Pc	33964		
His1	V27042		
His1	35205		
His1	44582		
His1	50723		
His1	54463		
His2A	35320		
His2B	41881		
His2B	41988		
His2AV	34844		
His2AV	44056		
His3	35344		
His3	41986		
His3.3A	N5825R3		
His3.3B	V12771		
His4	80366		
His4R	34816		
His4R	51172		

[a] RNAi lines are indicated by their BDSC, VDRC (V_) and NIG-FLY (N_) stock numbers.
[b] scored for expression in the apical tip of testes from *bamGAL4* adults
[c] scored for germline expression in testes from *bamGAL4* adults

Supplementary Table 3. Histone gene count tables.
Attached spreadsheet.

Key Resources Table

Reagent type	Designation	Source	Identifiers	Additional info
Antibody	anti-RNAPII (mouse)	Covance Research Products	MMS-126R	(1:100 CUT&Tag)
	anti-RNAPII-S5p (rabbit)	Cell Signalling Technology	D9N5I	(1:100 CUT&Tag)
	anti-RNAPII-S2p (rabbit)	Cell Signalling Technology	E1Z3G	(1:100 CUT&Tag)
	anti-Mxc (guinea pig)	RJ Duronio	Mxc-C-1	(1:100 CUT&Tag)
	anti-Mute (guinea pig)	RJ Duronio	Mute	(1:100 CUT&Tag)
	anti-H3K9me1 (rabbit)	Epicypher	13-0029	(1:100 CUT&Tag)
	anti-H3K9me2 (mouse)	EMD Millipore	05-1249	(1:100 CUT&Tag)
	anti-H3K9me3 (rabbit)	Abcam	ab8898	(1:100 CUT&Tag)
	anti-H3K27me3 (rabbit)	Cell Signalling Technology	C36B11	(1:100 CUT&Tag)
	anti-uH2A (rabbit)	Cell Signalling Technology	D27C4	(1:100 CUT&Tag)
	anti-H3K4me1 (rabbit)	Epicypher	13-0057	(1:100 CUT&Tag)
	anti-H3K4me2 (rabbit)	Epicypher	13-0027	(1:100 CUT&Tag)
	anti-H3K4me3 (rabbit)	Epicypher	13-0060	(1:100 CUT&Tag)
	anti-H3K27ac (rabbit)	Epicypher	13-0059	(1:100 CUT&Tag)
	anti-H3K36me3 (rabbit)	Epicypher	13-0058	(1:100 CUT&Tag)
	anti-MPM2 (mouse)	DAKO	M3514	(1:100 IF)
	anti-GFP (rabbit)	Cell Signalling Technology	D5.1	(1:100 IF)
	anti-GFP (mouse)	Thermo Fisher Scientific	3E6	(1:100 IF)
	anti-rabbit IgG (guinea pig)	Antibodies Online	ABIN101961	(1:100 CUT&Tag)
	anti-mouse IgG (rabbit)	Abcam	ab46540	(1:100 CUT&Tag)
	anti-guinea pig IgG (rabbit)	Thermo Fisher Scientific	PA1-28549	(1:100 CUT&Tag)
	anti-rabbit-FITC (goat)	Jackson ImmunoResearch	111-095-144	(1:200 IF)
	anti-mouse-FITC (goat)	Jackson ImmunoResearch	115-095-166	(1:200 IF)
	anti-mouse-RRX (goat)	Jackson ImmunoResearch	115-295-166	(1:200 IF)
	anti-mouse-Cy5 (goat)	Jackson ImmunoResearch	115-175-166	(1:200 IF)
	anti-guinea pig-TRITC (goat)	Jackson ImmunoResearch	706-025-148	(1:200 IF)
	anti-guinea pig-Cy5 (donkey)	Jackson ImmunoResearch	706-175-148	(1:200 IF)
	anti-histone H4 (mouse)	Abcam	ab31830	(1:200 IF)
	anti-histone H3-S10p (mouse)	Abcam	Ab14955	(1:5000 IF)
	anti-NPAT (rabbit)	Thermo Fisher Scientific	PA565419	(1:200 IF)

Genetic reagent (*D melanogaster*)	*w*^{1118}	BDSC	3605	
	12XWT	RJ Duronio		VK33 insert, MacKay et al 2015
	w ; ΔHisC ; 12XWT	RJ Duronio		MacKay et al 2015
	His2ADendra2	this paper		P40 insert
	His2ADendra2	this paper		VK33 insert
	His3Dendra2	A Amodeo		P40 insert, Shindo & Amodeo 2019
	His2AvDendra2	this paper		CRISPR integrant
	His3.3ADendra2	A Amodeo		CRISPR integrant, Shindo & Amodeo 2019
	bamGAL4	BDSC	80579	
	UASRFP	BDSC	30556	
	GFPMxc	B Duronio		White et al 2011
	UAS-H3-GFP	K Ahmad		Schwartz & Ahmad 2005
	UAS-H3.3-GFP	K Ahmad		Schwartz & Ahmad 2005
	UAS-H4-GFP	this paper		M1A insert
	Su(var)3-9^{1}	BDSC	6209	
	Su(var)3-9^{2}	BDSC	6210	
	GD-27042 (*His1* RNAi)	VDRC	27042	Dietzl et al 2007
	P[TRiP.GL00081]attP2 (*His1* RNAi)	BDSC	35205	
	P[TRiP.HMS02879]attP2 (*His1* RNAi)	BDSC	44582	
	P[TRiP.HMS02959]attP40 (*His1* RNAi)	BDSC	50723	
	P[TRiP.HMS03724]attP2 (*His1* RNAi)	BDSC	54463	
	P[TRiP.GL00226]attP2 (*His2A* RNAi)	BDSC	35320	
	P[TRiP.HMS02295]attP2 (*His2B* RNAi)	BDSC	41881	
	P[TRiP.HMS02387]attP40 (*His2B* RNAi)	BDSC	41988	
	P[TRiP.HMS00162]attP2 (*His2AV* RNAi)	BDSC	34844	
	P[TRiP.HMS02773]attP40 (*His2AV* RNAi)	BDSC	44056	
	P[TRiP.GL00255]attP2 (*His3* RNAi)	BDSC	35344	

	P[TRiP.HMS02385]attP40 (*His3* RNAi)	BDSC	41986	
	P[UAS-His3.3A-IR]5825R-3 (*His3.3A* RNAi)	NIG-FLY	5825R-3	
	GD-12771 (*His3.3B* RNAi)	VDRC	12771	
	P[TRiP.HMC06602]attP40 (*His4* RNAi)	BDSC	80366	
	P[TRiP.HMS00126]attP2 (*His4r* RNAi)	BDSC	34816	
	P[TRiP.HMJ21134]attP40 (*His4r* RNAi)	BDSC	51172	
	P[TRiP.HMS00279]attP2 (*Su(var)3-9* RNAi)	BDSC	33401	
	P[TRiP.GL01471]attP40 (*Su(var)3-9* RNAi)	BDSC	43661	
	P[TRiP.HMS00112]attP2 (*egg* RNAi)	BDSC	34803	
	P[TRiP.GL01002]attP40 (*egg* RNAi)	BDSC	36797	
	P[TRiP.HMS00066]attP2 (*E(z)* RNAi)	BDSC	33659	
	P[TRiP.GL00371]attP2 (*Sce* RNAi)	BDSC	35446	
	P[TRiP.HMJ23146]attP40 (*Sce* RNAi)	BDSC	61312	
	P[TRiP.HMS00278]attP2 (*HP1* RNAi)	BDSC	33400	
	P[TRiP.GL00531]attP40 (*HP1* RNAi)	BDSC	36792	
	P[TRiP.HMS01699]attP40 (*HP2* RNAi)	BDSC	38255	
	PcGFP	BDSC	9593	
	UAS-H4-eGFP	X Chen		Wooten et al 2019
Biological sample (*D melanogaster*)	Male larval wing imaginal discs	this paper		
	Male adult testes	this paper		
Biological sample (*H sapiens*)	K562 cell culture	ATCC	CCL-243	
Commercial reagent	pAGTn5	Epicypher	15-1017	
	EdU Click-iT kit	Invitrogen	C10340	
Software	bowtie2			
	bedtools/bamcoverage			
	subReads/featureCounts			